Earthquake Engineering, Tenth World Conference © 1992 Balkema, Rotterdam. ISBN 90 5410 060 5

# Amplitude of surface waves in ground motion on alluvial basin

J.Shibuya
*Tohoku University, Sendai, Japan*

ABSTRACT : The present study aims to make a quantitative evaluation of amplitudes of local surface waves in the ground motion in a sedimentary basin and to discuss the effects of various factors on the local surface wave amplitude. A method of evaluation of spectral amplitudes of surface waves extracted from results of the boundary element analysis on a sedimentary basin is proposed. Applying the method to the numerical results for the ground motion of a 2-dimensional shallow sedimentary basin subjected to incident SH waves, a smooth spectral amplitude curve of surface waves is obtained. The impedance contrast between the sediment and the underlying bedrock has a significant effect on the surface wave amplitude. The maximum spectral amplitude of surface waves of a sedimentary basin with a high impedance contrast reaches several times as large as that of a sedimentary basin with a low impedance contrast. The incident angle of the incident wave has a remarkable effect on the surface wave amplitude. The maximum surface wave amplitude in the case of 45° incident angle is about 1.6 times as large as that in the case of vertical incidence.

## 1 INTRODUCTION

Some strong ground motion records observed on extremely soft grounds during recent earthquakes, for example, a record on the reclamation dike at Hachirogata in Japan during the 1983 Mid-Japan Sea earthquake and some records in the Mexico city area during the 1985 earthquake, have attracted great attention of engineers and researchers of the earthquake engineering field because of their singular waveforms. They had monotonous sinusoidal waveforms with large amplitudes in the late parts of the records. This resulted in extraordinarily long durations of the ground motions.

It is considered that local surface waves play an important role in these features of the ground motions on alluvial basins. Bard and Bouchon (1980) calculated the ground motions of sedimentary basin models to the incident plane waves using the method proposed by Aki and Larner (1970) and showed that the local surface waves were generated at the lateral edges of the basin and propagated in the basin. Campillo *et al.*(1988) and Bard *et al.*(1988) examined the ground motions recorded in the Mexico city during the 1985 earthquake and pointed out that the effects of lateral heterogeneity of the valley on the ground motions were essential. Shibuya (1988) simulated the ground motion record observed on the reclamation dike during the 1983 Mid Japan Sea earthquake considering the local surface waves using the extended method proposed by Alsop (1966). The duration and the envelope shape of the simulated motion agreed well with the observed one. Shima *et al.* (1989), Kawase *et al.* (1989) and others simulated the ground motions in the Ashigara valley in Japan and discussed the effect of the 2-dimensional geological topography of the valley on the ground motion.

In this study, presented is a method to evaluate a local surface wave amplitude which is extracted from the numerical results of the boundary element analysis on a shallow alluvial basin model to incident plane waves. Moreover, using the method, effects of the geological configuration of a basin edge, the impedance contrast between the sediment and the underlying bedrock and the angle of incidence of incident waves on the local surface waves are investigated. These results will be useful for the interpretation of the complex characteristics of ground motions in soft sedimentary basins.

## 2 METHOD OF ANALYSIS

### 2.1 *Modeling of wave propagation in a basin*

Fig. 1 shows a 2-dimensional shallow sedimentary basin model subjected to incident plane SH waves. The response of the basin can be calculated by the numerical method such as the finite element method, the boundary element method, the Aki-Larner method and so on. First, we approximate the numerical results of the basin response as the sum of a body wave and two

surface wave components, as shown in Eq.(1).

$$F(x,\omega) \cong G(\omega)\exp[-ik_0x] + H_1(\omega)\exp[-ikx] + H_2(\omega)\exp[ikx] \quad (1)$$

where, $F(x,\omega)$ is the numerical frequency response at the position $x$ on the surface of the basin, $G(\omega)$ is the 1-dimensional response of the sediment regarded as laterally homogeneous, $H_1(\omega)$ and $H_2(\omega)$ are the amplitudes of the surface waves propagating in the positive and negative direction, respectively, $k_0$ is the wavenumber of the S-wave in the x-direction and $k$ is the wavenumber of the surface wave. $H_1(\omega)$ and $H_2(\omega)$ are unknown functions, now. In the case of vertical incidence, the response of the basin is symmetrical and can be approximated as the following.

$$F(x,\omega) \cong G(\omega) + 2H(\omega)\cos(kx) \quad (2)$$

Unknown complex surface wave amplitudes $H_1(\omega)$ and $H_2(\omega)$ can be determined so as to minimize $J$, defined in Eq.(3).

$$J = \Sigma\,[E(x_i)\cdot E^*(x_i)] \quad (3)$$

where $E(x_i)$ is a complex error due to the approximation of a ground motion in Eq.(1) or (2) at the discretized position $x_i$ of the basin surface. For the Eq.(3), the response of the discretized position within the central part of one wavelength of the Love wave of the basin are used.

Fig. 2 shows an example of the complex responses of a shallow sedimentary basin subjected to a vertical incident wave calculated by the method of boundary element. Dimensions and geological parameters are described in the figure. The response is symmetrical with respect to $x$=0. In the figure, also plotted is the 1-dimensional response $G(\omega)$ of the sediment by dotted lines. It is seen that the response $F(x,\omega)$ varies like a cosine function around $G(\omega)$, except for the response near the basin edge region. This fact supports the validity of the approximation in Eq.(2) for the ground motion in the central part of a shallow basin.

The velocity of the laterally propagating wave, which is obtained from the wavelength of the figure [$F(x,\omega)$-$G(\omega)$] of the central part of the basin, as shown in Fig. 2, is plotted in Fig. 3 by a circle. Theoretical Love wave velocity is also shown in the figure. It is proved that the main component of the laterally propagating wave is a Love wave from the fact that the dispersion characteristics of the laterally propagating wave agrees well with that of the Love wave.

### 2.2 *Direct and reflected surface waves*

An example of the spectral amplitude of the surface waves generated at the edge of the sedimentary basin

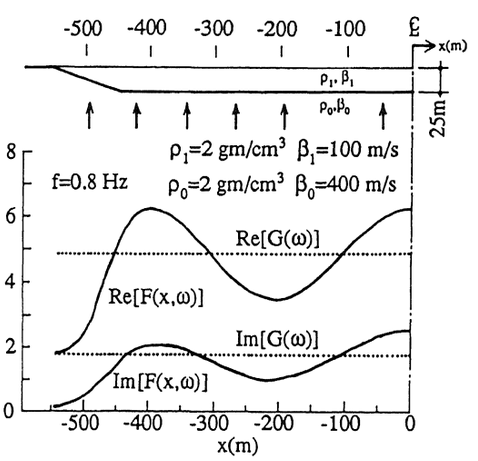


Fig. 2 Distribution of surface response of a basin.

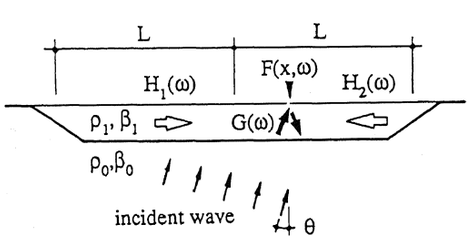


Fig. 1 Modelling of wave propagation in a basin.

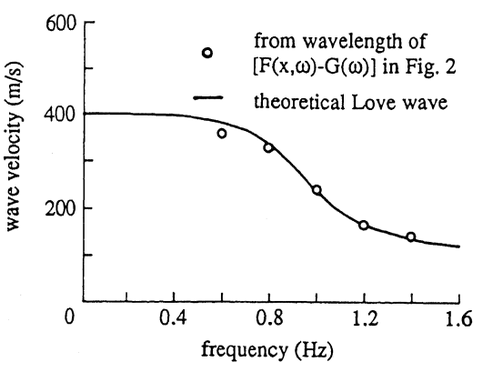


Fig. 3 Dispersion curve of surface wave.

model, which is evaluated by the method described in the previous section, is shown in Fig. 4 by a fine solid curve. Geological dimensions and parameters of the model and the angle of incidence re the same as those in Fig. 2. It is seen that the spectral amplitude fluctuates rapidly. This is considered to be caused by the fact that the expression of the surface wave amplitude in Eqs.(1) or (2) contains the surface waves reflected on the edge of a basin as well as the originally generated surface waves at the basin edge.

Next, therefore, we try to decompose the amplitude of surface waves expressed in Eqs.(1) and (2) into the originally generated surface wave (direct surface wave) amplitude and reflected surface wave amplitude. For the simplicity, only one-time reflection is considered in this study. The amplitude of surface waves, $H_1(\omega)$ and $H_2(\omega)$, propagating in the positive and negative direction, respectively, are decomposed as in Eqs.(4) and (5), considering the phase difference of the direct and the reflected surface waves.

$$H_1(\omega) \cong H_{1D}(\omega)\exp[i(k_0-k)L] + H_{1R}(\omega)\exp[-i(k_0+3k)L] \quad (4)$$

$$H_2(\omega) \cong H_{2D}(\omega)\exp[-i(k_0+k)L] + H_{2R}(\omega)\exp[i(k_0-3k)L] \quad (5)$$

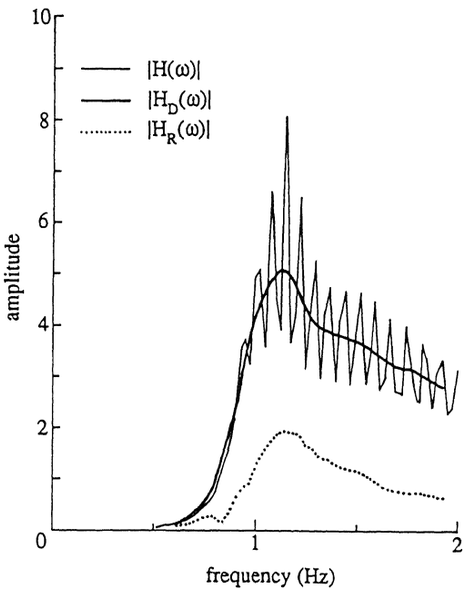


Fig. 4 Comparison of amplitudes between non-decomposed and decomposed surface waves.

where $H_D(\omega)$ and $H_R(\omega)$ are the direct and the reflected surface wave amplitudes, respectively, and $L$ is a length of a basin. In Eqs.(4) and (5), the exponential functions oscillate rapidly because of the large value of $L$ in the shallow sedimentary basin case. Assuming $H_D(\omega)$ and $H_R(\omega)$ as constants within a narrow frequency band (0.2 Hz, in this study), $H_D(\omega)$ and $H_R(\omega)$ can be obtained using the least absolute square error method. An example of decomposed surface wave amplitudes $H_D(\omega)$ and $H_R(\omega)$ are also shown in Fig. 4 by a thick solid curve and a dotted curve, respectively. It is proved that the decomposed spectral amplitudes of surface wave are very smooth compared with the non-decomposed surface wave amplitudes. It is considered that the decomposed spectral amplitude is reliable for the following investigation on the local surface wave.

## 3 RESULTS AND DISCUSSIONS

### 3.1 *Cases studied*

Studied cases of sedimentary basin models are summarized in Table 1. A length, $L$, and a depth, $H$, of a basin is fixed as 1km and 25m, respectively. Shear wave velocity of the sediment, $\beta_1$, is also fixed as 100 m/s. Densities of both the sediment and the bedrock, $\rho_1$ and $\rho_0$, are 2 gm/cm$^3$.

Table 1 Studied cases for sedimentary basin models.

| symbol | shape of edge | velocity of bedrock $\beta_0$ | incident angle $\theta$ |
|---|---|---|---|
| A-200-0<br>A-300-0<br>A-400-0 | type-A<br>d=100m | 200m/s<br>300m/s<br>400m/s | 0° |
| B-400-0 | type-B<br>d=50m | 400m/s | 0° |
| C-400-0 | type-C | | |
| A-400-22<br>A-400-45 | type-A | 400m/s | 22.5°<br>45° |

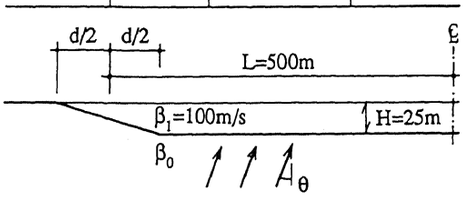

The shear wave velocity of the bedrock, the geometrical shape of the basin edge and the angle of incidence are varied as shown in Table 1 in order to investigate their effects on the local surface wave amplitude. Three cases for the bedrock shear wave velocity $\beta_0$, 200 m/s, 300 m/s and 400 m/s, are studied. Three types of geometrical shape of the basin edge, type-A, type-B and type-C, are studied. Three cases of incident angle of the incident wave, 0°, 22.5° and 45° are studied.

### 3.2 *Effect of shear wave velocity contrast*

Figs. 5, 6 and 7 show the spectral amplitudes of local surface waves for the various shear wave velocity of bedrock. In these analyses, the shape of basin edge and the incident angle are taken to be common, that is to say, type-A edge shape and vertical incidence. In these figures, 1-D response amplitudes of laterally homogeneous layered media are also shown by dotted curves.

It is seen that a local surface wave hardly appears in the frequency range lower than about 0.6 Hz and grows in its amplitude suddenly near the frequency around the fundamental resonant frequency of the sediment, 1Hz. The frequency at which the amplitude of the surface wave takes the maximum value is somewhat higher than the fundamental resonant frequency of the sediment. It is also proved that the amplitudes of surface waves increase with the increase in the shear wave velocity ratio $\beta_0/\beta_1$. The maximum amplification of the local surface wave reaches about 5 in the case of high shear wave velocity ratio of $\beta_0/\beta_1=4$, whereas the maximum amplification of the local surface wave is merely around 1 in the case of low velocity ratio of $\beta_0/\beta_1=2$.

### 3.3 *Effect of shape of basin edge*

Fig. 8 shows the comparison of the surface wave amplitudes among the models with various shapes of basin edge, shown in Table 1. In these analyses, the bedrock shear wave velocity and the angle of incidence remain constant, 400 m/s and 0°,respectively. It is found that the shape of basin edge has few effects on the amplitude of local surface waves because the three curves in Fig. 8 are almost similar to each other.

### 3.4 *Effect of incident angle*

Figs. 9 and 10 show the surface wave amplitudes for the incident angle of 22.5° and 45°, respectively, of the model with the 400 m/s bedrock shear wave velocity and with the type-A basin edge shape. In these figures, the amplitudes for two kinds of surface waves are plotted. One is for the surface waves which are generated at the left-hand basin edge, first reached by the incident

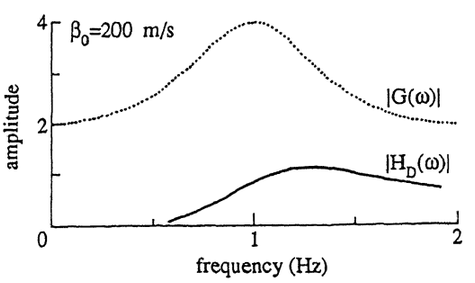


Fig. 5 Amplitude of surface wave (A-200-0) and 1-D response.

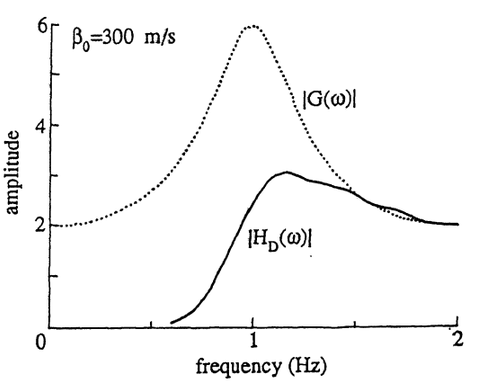


Fig. 6 Amplitude of surface wave (A-300-0) and 1-D response.

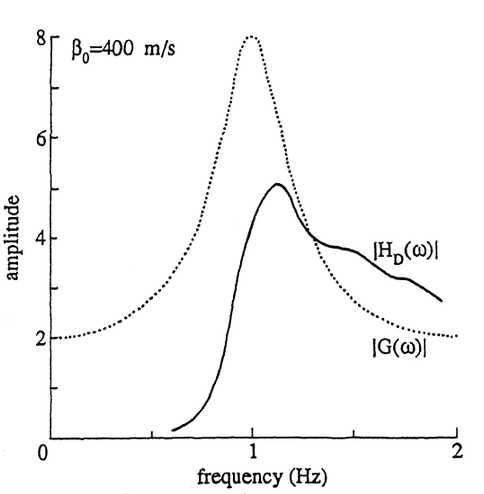


Fig. 7 Amplitude of surface wave (A-400-0) and 1-D response.

wave, and propagate in the positive x direction, $H_{1D}(\omega)$ in Eq.(4). The other is for the surface waves which are generated at the right-hand basin edge and propagate in the negative x direction, $H_{2D}(\omega)$ in Eq.(5). The surface wave amplitudes for the vertical incidence is shown in Fig. 7. It is found that the amplitude of the surface wave propagating in the positive direction is larger than that of the surface wave propagating in the negative direction in the case of oblique incidence. This tendency is stressed by the increase in the angle of the incident wave.

Fig. 11 shows the comparison of the surface wave amplitudes propagating in the positive direction among the cases of incident angles of 0°, 22.5° and 45°. The amplitude increases significantly as the incident angle increases. The maximum surface wave amplitude in the case of 22.5° incident angle is about 1.2 times, and that in the case of 45° incident angle is about 1.6 times as large as that in the case of vertical incidence. The frequency at which the amplitude indicates the maxi-

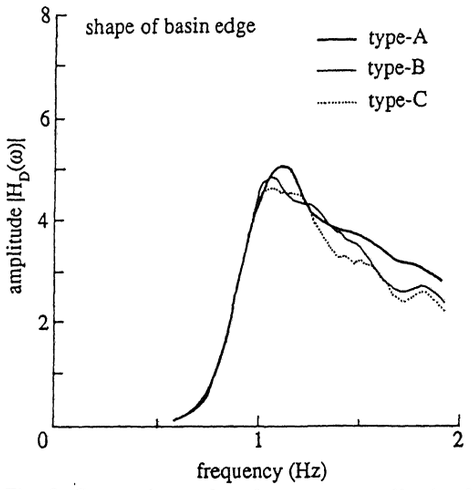


Fig. 8 Comparison of surface wave amplitudes for various shapes of basin edge.

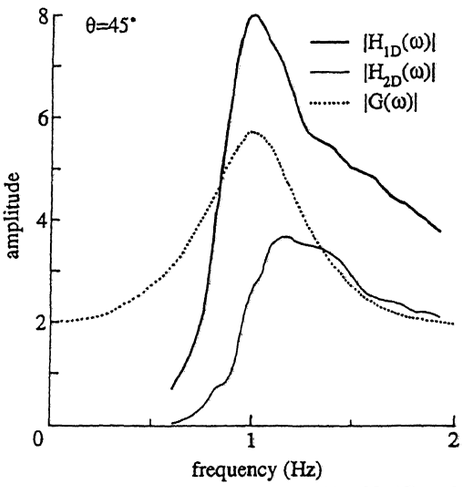


Fig. 10 Amplitude of surface wave (A-400-45) and 1-D response.

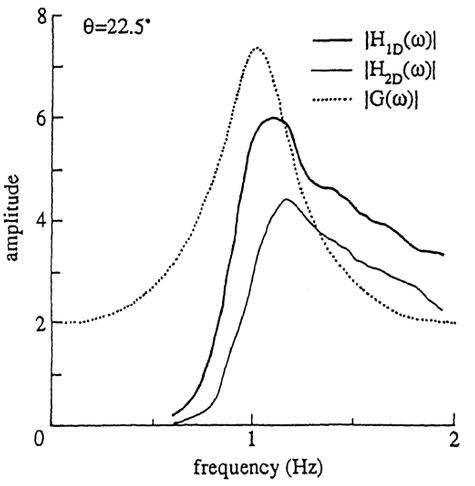


Fig. 9 Amplitude of surface wave (A-400-22) and 1-D response.

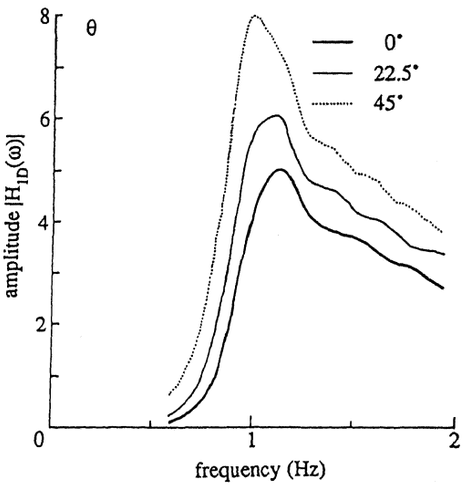


Fig. 11 Comparison of surface wave amplitudes for various incident angle.

mum shifts to the lower side as the incident angle increases.

## 4 CONCLUSIONS

First, a method for the evaluation of spectral amplitude of local surface waves extracted from the results of total wave field analysis on the 2-dimensional shallow sedimentary basin model subjected to plane SH wave is proposed. Obtained spectral amplitudes, using the method, of the surface waves are smooth enough to examine the effects of various factors on the amplitude of surface waves.

Next, the effects of geological configuration, the impedance contrast between the sediment and the underlying bedrock and the angle of incidence of the incident wave on the amplitude of local surface waves in a shallow sedimentary basin are discussed. Amplitudes of local surface waves are small in the lower frequency than the fundamental resonant frequency of the sediment and become remarkably large near the resonant frequency. The maximum spectral amplitude occurs at the frequency 10 to 20% higher than the fundamental resonant frequency of the sediment. The impedance contrast has a significant effect on the amplitude of surface waves. A higher impedance contrast results in a larger surface amplitude. For example, the maximum amplification of the surface wave reaches to about 5 in the case of velocity contrast $\beta_1/\beta_0=4$, whereas the maximum amplification of the surface wave is only around 1 in the case of the velocity contrast $\beta_0/\beta_1=2$. The ratio of the maximum amplitude of the surface wave to the maximum amplitude of the 1-D response is about 0.63 in the case of velocity contrast $\beta_1/\beta_0=4$ and vertical incidence.

For the examination of the effect of basin edge shape, the surface wave amplitude of three basin models, of which lateral edges have different slopes, 1/4, 1/2 and vertical, are studied. It is proved that the shape of basin edge has few effects on the amplitude of the local surface waves in the case of vertical incident wave because the curves of the spectral amplitude of surface waves for the three cases are almost similar to each other.

For the examination of the incident angle of incident wave on the amplitude of local surface waves, three cases of the incident angle, 0°, 22.5° and 45°, are studied. The surface wave amplitude increases significantly as the incident angle increases. For example, the surface wave amplitude in the case of 45° incident angle is about 1.6 times as large as that in the case of vertical incident. It is also shown that the amplitude of surface wave propagating in the positive direction is larger than that propagating in the negative direction. These tendency is stressed by the increase in the incident angle.

Finally, the results of the present study on the amplitude of the local surface wave will provide useful information for engineers and researchers in making the interpretation of complex ground motions, or predicting ground motions in a soft sedimentary basin.

## REFERENCES


Aki, K. and K.L. Larner 1970. Surface motion of a layered media having an irregular interface due to incident plane SH waves. *Jour. Geophys. Res.*, vol.75 : 933-954

Alsop, L.E. 1966. Transmission and reflection of Love waves at vertical discontinuity. *Jour. Geophys. Res.*, vol.71, : 3969-3984

Bard, P.-Y and M. Bouchon 1980. The seismic response of sediment-filled valleys. Part 1. The case of incident SH waves. *Bull. Seism. Soc. Am.*, 70, No.4 : 1263-1286

Bard, P.-Y, M. Campillo, F. Nicollin and F.J. Sanchez-Sesma 1988. A theoretical investigation of large and small-scale amplification effects in the Mexico City valley. *Earthquake Spectra*, vol.4, No.3 : 609-633

Campillo, M., P.-Y. Bard, F. Nicollin and F.J. San chez-Sesma 1988. The incident wave field in Mexico City during the great Michoacan earthquake and its interaction with the deep basin. *Earthquake Spectra*,vol.4, No.3 : 591-608

Kawase, H., T. Sato, T. Watanabe, H. Yokota S. Kataoka 1989. Synthetics of strong ground motion considering diffracted waves generated at the edges of the basin. *Proc. National Symposium on the Effects of Surface Geology on Seismic Motion*, Japanese WG on ESG on Seismic Motion : 299-310

Shibuya, J. 1988. Analysis of ground motions on alluvial deposit considering surface waves. *Proc. the Ninth world Conf. on Earthquake Eng.*, 2 :551-556

Shima, E., T. Ohta, M. Inou, M. Motosaka, H. Ishida and K. Kamata 1989. Earthquake response characteristics of Ashigara valley by discrete wave number method. *Proc. National Symposium on the Effects of Surface Geology on Seismic Motion*, Japanese WG on ESG on Seismic Motion : 299-310